Science of the Total Environment 754 (2021) 142247

Contents lists available at ScienceDirect

Science of the Total Environment

journal homepage: www.elsevier.com/locate/scitotenv

# A calibration of cellulose isotopes in modern prostrate *Nothofagus* and its application to fossil material from Antarctica

Rhian L. Rees-Owen [a,1], Robert J. Newton [a,*], Ruza F. Ivanovic [a], Jane E. Francis [b], James B. Riding [c], Alina D. Marca [d]

[a] School of Earth and Environment, University of Leeds, Leeds, UK
[b] British Antarctic Survey, Cambridge, UK
[c] British Geological Survey, Nottingham, UK
[d] School of Environmental Sciences, University of East Anglia, Norwich, UK

## HIGHLIGHTS

- Prostrate trees record average climate over decadal time periods in tree ring cellulose-$\delta^{18}O$.
- Late Neogene Antarctic wood indicates a ~12‰ enrichment in $H_2O$-$\delta^{18}O$ relative to today.
- Evidence for marked changes in Antarctic hydrological cycle

## GRAPHICAL ABSTRACT

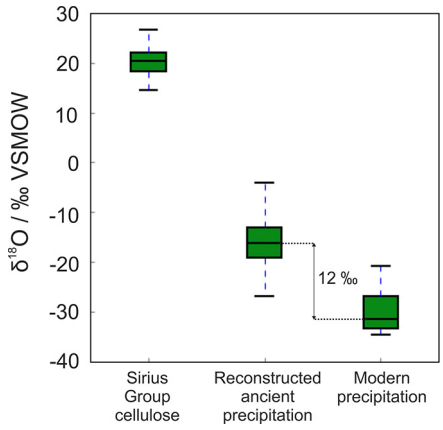


## ARTICLE INFO

*Article history:*
Received 28 February 2020
Received in revised form 21 August 2020
Accepted 4 September 2020
Available online 7 September 2020

Editor: Raul Sanchez-Salguero

*Keywords:*
Antarctica
Neogene
Sirius Group
Tree ring isotopes
Precipitation

## ABSTRACT

Carbon and oxygen isotopes ($\delta^{13}C$ and $\delta^{18}O$) in tree rings are widely used to reconstruct palaeoclimate variables such as temperature during the Holocene (12 thousand years ago - present), and are used increasingly in deeper time. However, their use is largely restricted to arboreal trees, which excludes potentially important data from prostrate trees and shrubs, which grow in high latitude and altitude end-member environments. Here, we calibrate the use of $\delta^{13}C$ and $\delta^{18}O$ as climatic archives in two modern species of southern beech (*Nothofagus*) from Tierra del Fuego, Chile, at the southern limit of their current range. We show that prostrate trees are potentially suitable archives for recording climatological means over longer periods (on the order of decades), which opens up these important environments for tree ring isotope analysis. We then apply our new understanding to a remarkable late Neogene (17–2.5 Ma) fossil *Nothofagus* assemblage from the Transantarctic Mountains, Antarctica, representative of a prostrate tundra shrub growing during a period of significant ice sheet retreat. The $\delta^{13}C$ of the fossil cellulose was found to be ~4‰ enriched relative to that of the modern tress. This is likely to be due to a combination of a more positive $\delta^{13}C$ of contemporaneous atmospheric $CO_2$ and enhanced water use efficiency at the fossil site. Using the cellulose-$\delta^{18}O$ in the fossil wood, we are able to reconstruct precipitation oxygen isotopes over the Antarctic interior for the first time for this time period. The results show that $\delta^{18}O_{precip}$ over Antarctica was $-16.0 \pm 4.2$‰, around 12‰ enriched relative to today, suggesting changes in the hydrological cycle linked to warmer temperatures and a smaller ice sheet.

© 2020 The Authors. Published by Elsevier B.V. This is an open access article under the CC BY license (http://creativecommons.org/licenses/by/4.0/).

* Corresponding author.
*E-mail address:* r.j.newton@leeds.ac.uk (R.J. Newton).
[1] Present address: Department for Business, Energy, and Industrial Strategy, 1 Victoria St, Westminster, London SW1H 0ET.

https://doi.org/10.1016/j.scitotenv.2020.142247
0048-9697/© 2020 The Authors. Published by Elsevier B.V. This is an open access article under the CC BY license (http://creativecommons.org/licenses/by/4.0/).

## 1. Introduction

Tree ring stable isotope analysis is a powerful and widely-used tool for palaeo-climatic reconstructions (Cernusak and English, 2014; Gessler et al., 2014). It can provide rare insights into terrestrial palaeoclimate and environmental evolution at high temporal resolution, providing information on temperature (Gagen et al., 2007; Naulier et al., 2014; Lavergne et al., 2016, 2018), precipitation (Cullen and Grierson, 2009; Xu et al., 2016), drought (Kress et al., 2010; Labuhn et al., 2016), and large-scale atmospheric circulation patterns (Xu et al., 2013; Grießinger et al., 2018).

A key source of information in much of this work is the oxygen isotopic composition of tree ring cellulose ($\delta^{18}O_{cell}$). The theory on the underpinning variables controlling $\delta^{18}O_{cell}$ is relatively well developed, albeit with large uncertainties and knowledge gaps e.g. (Gessler et al., 2014; Treydte et al., 2014). The relationship between these variables and $\delta^{18}O_{cell}$ can be described by various numerical models and used to investigate oxygen isotope variations in multiple settings (Roden and Ehleringer, 2000; Farquhar and Gan, 2003; Ogée et al., 2003, 2009; Danis et al., 2012; Lavergne et al., 2017b). Cellulose oxygen isotopes are governed by a complex array of factors, including source water isotopic composition (itself a result of precipitation isotopes, soil residence time, and evaporative effects); leaf water enrichment due to transpiration (Yakir and Sternberg, 2000); fractionation between leaf water and carbonyl oxygen (Sternberg and DeNiro, 1983; Sternberg and Ellsworth, 2011); and other oxygen exchange processes between organic compounds and surrounding water, for example during remobilisation of organic matter or cellulose biosynthesis (e.g. Hill et al., 1995; Sternberg et al., 2006; Gessler et al., 2007; Offerman et al., 2011; Nabeshima et al., 2018). The underpinning link with source water oxygen isotopes means that tree-ring cellulose $\delta^{18}O$ can be used to reconstruct the oxygen isotopic composition of precipitation. This in itself is a function of precipitation amount, altitude, temperature, residence time in the atmosphere, distance from moisture source and transport patterns (Dansgaard, 1964; Sime et al., 2009; Aggarwal et al., 2012). Cellulose $\delta^{18}O$ can therefore be used as a proxy for reconstructing global and regional hydrological change, for example, changes in basinal water regimes (Brienen et al., 2012) or large-scale atmospheric circulation patterns (Baldini et al., 2008; Zhu et al., 2012).

Carbon isotopes in tree-ring cellulose ($\delta^{13}C_{cell}$) also have utility as a palaeoclimatic proxy. In general, $\delta^{13}C_{cell}$ is controlled by the $\delta^{13}C$ of atmospheric $CO_2$ (McCarroll and Loader, 2004; Treydte et al., 2007); atmospheric $CO_2$ concentrations (Beerling, 1996; Köhler et al., 2010; Battipaglia et al., 2013), along with other factors that affect stomatal conductance including soil moisture and atmospheric vapour pressure deficit; and factors that control photosynthetic capacity such as nutrient availability and irradiance (Ehleringer et al., 1986; Farquhar et al., 1989; Cernusak et al., 2007; Cernusak et al., 2009). A range of downstream metabolic processes also play a role in shaping $\delta^{13}C_{cell}$, including post-carboxylation fractionation, phloem loading and transport, and respiratory isotope fractionation (Gessler et al., 2009; Priault et al., 2009; Werner and Gessler, 2011; Werner et al., 2011).

Both carbon and oxygen tree ring isotopes are increasingly being applied to older time periods of up to 53 Ma as more fossil plants with adequate preservation are being recovered (Jahren and Sternberg, 2008; Schubert and Jahren, 2011; Schubert et al., 2012; Wolfe et al., 2012; Hare et al., 2018). One particular advantage of this growing dataset is the ability of tree ring isotopes to reconstruct climatic parameters that are much harder to access through marine sediments. These include environmental geochemical signals like precipitation isotopes (Ballantyne et al., 2006; Jahren and Sternberg, 2008; Jahren et al., 2009) and atmospheric carbon isotopes (Arens et al., 2000; Jahren et al., 2001). A notable example is the rich treasure trove of exceptionally well-preserved Eocene and Pliocene fossil wood from multiple kimberlite deposits in the Canadian High Arctic. These fossil recoveries have revealed unique details about Eocene and Pliocene palaeoclimate and hydrological cycling through their stable isotope records, such as reconstructing terrestrial temperatures and the isotopic composition of precipitation as well as providing insights into high latitude climate variability (Ballantyne et al., 2006, 2010; Jahren and Sternberg, 2008; Jahren et al., 2009; Csank et al., 2011; Wolfe et al., 2012).

In this study, we apply tree ring isotope analysis to a unique suite of fossil prostrate or *krummoltz Nothofagus* trees recovered from the mid-late Neogene (~17–2.5 Ma) Sirius Group deposits at the Oliver Bluffs in the Transantarctic Mountains, Antarctica (85°07′S, 166°35′E; Webb and Harwood, 1987, 1993; Francis and Hill, 1996; Hill et al., 1996). The plants were deposited at a similar latitude to today (Lawver and Gahagan, 2003) and represent a period of significant Antarctic Ice Sheet retreat, where warming of the continent allowed a tundra-like shrub to grow 480 km from the South Pole.

Based on both geochemical (Rees-Owen et al., 2018) and macrofossil-derived (Francis and Hill, 1996; Ashworth and Cantrill, 2004) palaeothermometers, continental summer temperatures during the trees' lifetimes were ~5 °C, implying a weakened latitudinal temperature gradient compared to the present day, where the mean temperature in December is −3.4 °C (McMurdo Station; 77°51′S, 166°40′E). Shallower gradients are also supported by vegetation and marine proxy-based reconstructions, indicating, for example, a reduction of ~5.5 °C in the meridional temperature gradient during the early Pliocene relative to today (Brierley et al., 2009; Pound et al., 2012).

The age of these sediments has been the subject of a lengthy debate, relating to the nature of the East Antarctic Ice Sheet under warmer-than-present conditions (Barrett, 2013). Biostratigraphical dating of the plant fossils by association with late Pliocene marine diatoms (Webb et al., 1984; Harwood, 1986) suggests the incursion of seaways deep into the Antarctic interior and indicates a dynamic ice sheet as late as 3 million years ago. This relatively young age for the plant fossils has been challenged by suggestions that the diatoms represent wind-blown contamination from the open ocean (Burckle and Potter, 1996; Stroeven et al., 1996). Furthermore, cosmogenic exposure dating of nearby moraines indicates these sediments are much older (at least 5 Ma, but possibly as old as 17 Ma; Ackert Jr. and Kurz, 2004) and therefore that the ice sheet has been a stable climatic feature since the mid-Miocene. Evidence for a periodically reduced ice sheet accompanied by vegetation along the margins exists for the mid-Miocene (17–15 Ma; Warny et al., 2009; Feakins et al., 2012; Griener et al., 2015; Gasson et al., 2016; Levy et al., 2016). Increasingly both modelling (Dolan et al., 2011; Austermann et al., 2015; Pollard et al., 2015; Pollard and Deconto, 2016) and data (Fielding et al., 2012; Cook et al., 2013; Ohneiser et al., 2020) studies also suggest that at least partial EAIS retreat occurred during the Pliocene, allowing a tundra shrub to grow around 4.1 Ma. These competing scenarios pose a challenge to dating these fossils. Nevertheless, the fossiliferous bed clearly represents a period of significant East Antarctic Ice Sheet (EAIS) retreat in response to warming temperatures (Mercer, 1986; Francis and Hill, 1996). Our data will therefore give novel insight into past Antarctic climate change during a vital period in its glacial history.

To date, the vast majority of tree ring stable isotope studies have been applied to trees with an arboreal habit. Prostrate trees (where stems grow horizontally to avoid harsh conditions such as freezing winds e.g. *Salix arctica* in the High Arctic and the fossil plants considered in this study) and shrubs are increasingly used in modern dendrochronological studies (Woodcock and Bradley, 1994; Hantemirov et al., 2011; Buras and Wilmking, 2014), where they can provide vital information on past climate for tree-less regions such as those at high latitude or altitude, and deserts. However, to our knowledge, no studies using tree ring isotopes in prostrate plants to reconstruct past climate exist, so there is uncertainty over the extent to which isotope theory developed for arboreal tree rings holds true for *krummholz*-type plants. Therefore, the objective of the first part of this study is to calibrate the

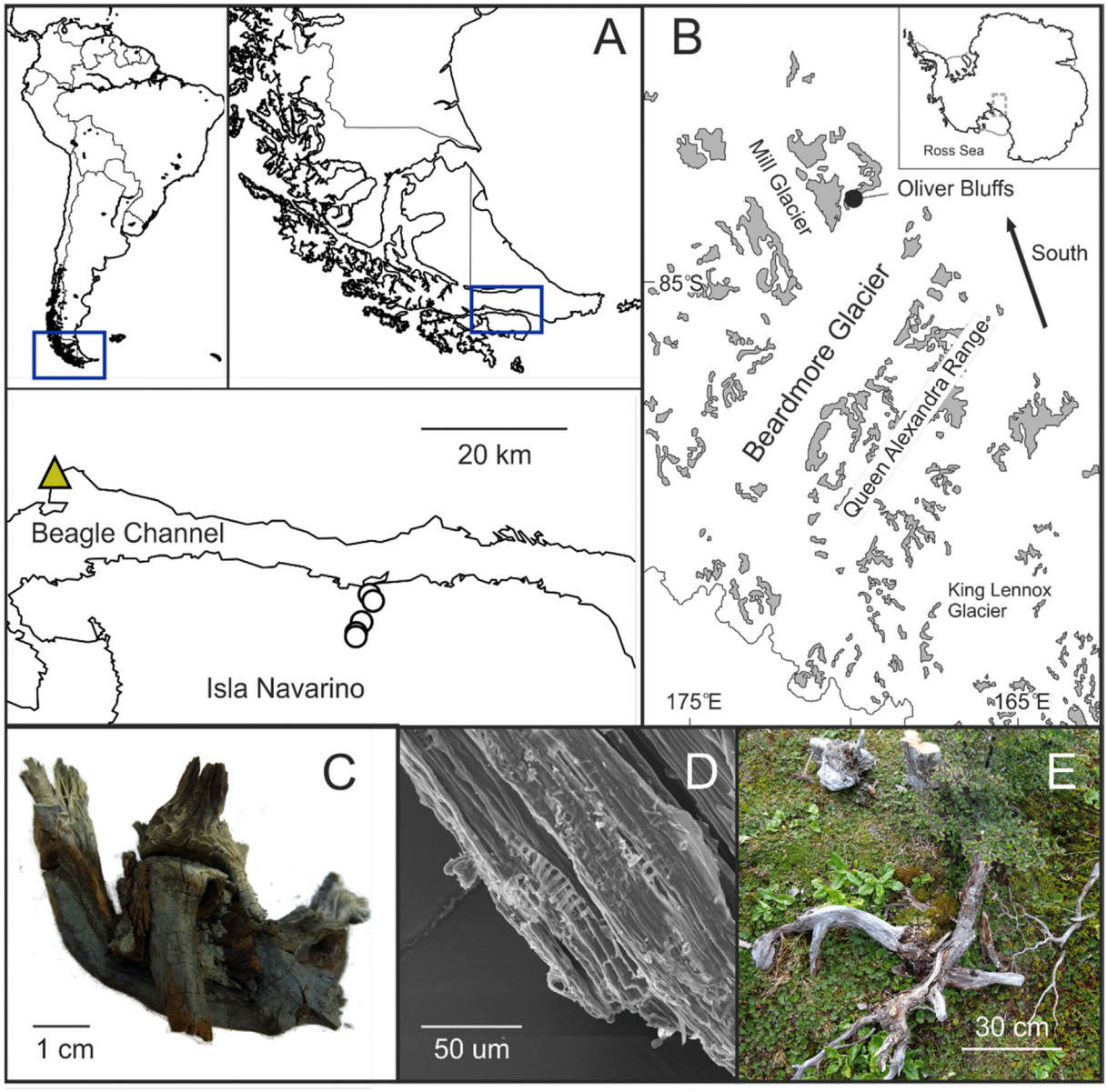


**Fig. 1.** (A) Location of sampling sites on Isla Navarino in Tierra del Fuego, Chile. Yellow triangle = marks the location of the GNIP station at Ushuaia; open circles = mark the tree ring sampling sites. (B) Fossil wood location at Oliver Bluffs (black filled circle), Transantarctic Mountains, Antarctica. White represents ice; grey shapes are Transantarctic Mountain outcrops. (C) Photograph of exceptionally preserved fossil Nothofagus from Oliver Bluffs. (D) Scanning Electron Microscope image of fossil *Nothofagus*, demonstrating excellent preservation of wood fibres. (E) Prostrate *Nothofagus antarctica* from Isla Navarino. (For interpretation of the references to colour in this figure legend, the reader is referred to the web version of this article.)

use of tree ring isotopes ($\delta^{13}C$ and $\delta^{18}O$) in high latitude prostrate trees for climatic reconstructions using plants from Isla Navarino, Chile, where two deciduous southern beech (*Nothofagus*) species grow in both arborescent and prostrate form in a subpolar forest environment at the southern limit of their range. The objective of the second part is to apply this new knowledge to our fossil *Nothofagus* trees to enhance our understanding of how the Antarctic Ice Sheet has behaved during past warm periods of Earth's history.

## 2. Materials and methods

### 2.1. Oliver Bluffs; fossil site

The fossil wood was sampled from a sedimentary succession at Oliver Bluffs in the Dominion Range of the Transantarctic Mountains (85°07′S, 166°35′E), which forms part of the Sirius Group sediments (Fig. 1). The fossil plant material occurs within one main bedding horizon in the central part of the exposure at Oliver Bluffs, on the eastern side of the upper valley of the Beardmore Glacier. The present elevation is approximately 1760 m above sea level, but deposition likely occurred at a much lower altitude (Webb and Harwood, 1993; Ackert Jr. and Kurz, 2004). The sedimentary sequence consists of glacial diamictites, and are thought to be lodgement tills deposited by the ancestral Beardmore Glacier during glacial advance and retreat (McKelvey et al., 1991). The fossiliferous bed containing fossil wood and leaves comprises poorly-sorted sandstones with silt lenses, representing an outwash deposit, in places burying poorly-developed glacial soils on a braided outwash plain (Ashworth and Cantrill, 2004). We envisage sporadic accretion of sediment over the plain, such that the fossiliferous bed is spatially heterogeneous, but as a whole is representative of a significant portion of the ice sheet retreat event (Rees-Owen et al., 2018).

The fossil wood fragments were first described as *Nothofagus* (Carlquist, 1987) and later identified as *Nothofagus beardmorensis* and are dated to between 17 and 2.5 Ma (Hill and Jordan, 1996; Hill et al., 1996). Leaf remains and tree ring analyses suggest that these were deciduous prostrate shrubs, very similar to the *krummholz N. pumilio* and *N. antarctica*, which grow at the treeline in Tierra del Fuego, Chile (Francis and Hill, 1996). Due to the small ring size (<100 μm) and friability of the material, fossil wood fragments were sampled for isotope analysis in bulk or by isolating individual rings where possible, so our measurements are averages over multiple years and up to several decades. The necessity of combining multiple rings together for the analysis of the fossil wood material sets the context for the modern part of our study in which we stress the interpretation of data on decadal rather than annual timescales.

### 2.2. Isla Navarino; modern analogue site

Isla Navarino (55°56′S, 67°37′W; Fig. 1) is part of the Magellanic subpolar forests ecoregion which stretches west of the Andes down to Tierra del Fuego, Chile. The island has a maritime climate, with mean annual temperatures of 6 °C, average summer highs of 10 °C and winter averages of 2 °C. Cool windy conditions prevail year round; Mean Annual Precipitation (MAP) is 400–500 mm, which is uniformly distributed throughout the year. The island vegetation is characterised by Magellanic forest dominated by *Nothofagus* trees to the north, and Magellanic moorland to the south.

The overall intention of this study is to ascertain whether the Antarctic fossil trees can be used for tree ring isotope work, so we designed our sampling strategy for the modern plants to mimic this where possible, including limiting our study to *Nothofagus* only. Wood cores and rounds from branches (for prostrate trees) from 31 living trees were collected at five sites on Isla Navarino during the austral summer of 2013. Three species of *Nothofagus* trees grow on the island, one evergreen species (*N. betuloides*) and two deciduous species (*N. antarctica* and *N. pumilio*). Because the fossil *Nothofagus* from the Sirus Group sediments are deciduous (Hill et al., 1996), cores were taken from two deciduous *Nothofagus* species over an altitude transect from near sea-level to the treeline (~600 m) at 5 sites (Table 1; Fig. 1). Over the transect, *Nothofagus* ranged in habit from arborescent (single stem and generally greater than 4 m in height) to *krummholz* form (i.e. prostate, with a small trunk or stem and multiple branches lying horizontally upon the ground). Species were identified by leaf character (Moore, 1983) and sampled during the height of austral summer 2013 (January), when the trees were in full leaf. Arborescent trees were cored at chest height (~130 cm above the ground) using an increment wood corer with a diameter of 5 mm. Prostrate individuals were sampled from primary branches in order to match sampling from the fossil trees. Two cores or rounds were sampled per individual tree and the cores and rounds were air-dried; cores were stored in plastic straws. Rounds were sanded with progressively fine sandpaper, and the surface of the tree-ring cores were cut using a core-microtome to improve ring visibility.

The core samples were dated to the calendar year of their formation and cross-dated using the techniques described in (Stokes and Smiley, 1968). These were then statistically tested using the programme COFECHA (Holmes, 1983; Grissino-Mayer, 2001) and chronologies were constructed using ARSTAN (version 44h3; Cook and Krusic, 2014). As the austral growing season overlaps two calendar years, rings were assigned to the year when ring growth began (i.e. the last complete ring taken for each core in January 2013 was dated to austral summer 2011, as the 2012–2013 ring was still incomplete at the time of sampling).

A 30 year sequence was isolated for isotopic analysis covering the period 1981–2011. This sequence length was chosen to roughly match the available tree ring spans of the fossil trees sampled here. Tree rings are composed of earlywood and latewood; the former comprises large thin-walled cells made of stored photosynthates from the previous year and the latter comprises thicker-walled cells formed during summer. Therefore to sample at true annual resolution, it has been suggested that only latewood should be taken (Switsur et al., 1995). However, the rings in the prostrate plants in this study were too small to obtain sufficient latewood, so the entire ring was sampled each time; this approach has been used successfully to reconstruct temperature in the same region (Lavergne et al., 2016). Isotope ratios were measured separately for each year and each tree. There are multiple missing years in the isotope chronologies where rings were too small to extract sufficient cellulose for analysis.

Chronologies at annual resolution require the construction of chronologies that are statistically representative of the variability of the site. An Expressed Population Signal (EPS; Wigley et al., 1984) was calculated for each site's $\delta^{18}O$ and $\delta^{13}C$ chronologies. This is a measure of how well a chronology constructed from a finite number of trees represents the hypothetical perfect or true chronology; a value of 0.85 is generally considered to be an acceptable confidence level. On the whole, EPS is highly sensitive to the number of trees in the chronology. In this study, the EPS for each site was low (particularly for $\delta^{13}C$) (0.65–0.87 for $\delta^{18}O$; 0.46–0.76 for $\delta^{13}C$), suggesting that a greater sample size is needed to be representative of the whole sample site, particularly for $\delta^{13}C$, which generally exhibits lower EPS (Daux et al., 2018). Because we are not intending to develop a detailed chronology for Isla Navarino, but instead test whether tree ring isotopes are broadly applicable to our prostrate fossil trees, we judge that this is adequate for the purposes of this study.

Soil and root samples were also collected, along with water from a stream network covering the altitude transect in order to estimate source water $\delta^{18}O$. Soils were sampled from 50 cm depth around the roots of three trees from each of the five sites (where 90% of *Nothofagus* forest root mass is situated; Schulze et al., 1996). Root samples were taken from at least one tree at three of the five sites. Roots and soils were wrapped in cling film, stored in multiple airtight bags and frozen until required for water extraction. Source water samples were taken from seven fast-flowing streams and one lake, covering the entire altitudinal transect, filtered (0.2 μm), and stored in McCartney vials.

### 2.3. Sample preparation and isotopic analysis

Except where otherwise indicated, the following procedures were all carried out in the University of Leeds Cohen Geochemistry laboratories in the School of Earth and Environment, 2013–2016.

Oxygen isotope ratios are expressed as $\delta^{18}O$; where delta notation is the conventional notation used for the ratio of isotopes (e.g. $^{18}O/^{16}O$) in a sample (R) relative to a standard ($R_{STD}$) such that $\delta = (R/(R_{STD} - 1)\ 1000)$ reported in per mil (‰). Results are reported with respect to Vienna Standard Mean Ocean Water (VSMOW). Carbon isotope ratios

**Table 1**
Summary of sample sites on Isla Navarino with mean site $\delta^{18}O_{soil}$.

| Site | Latitude | Longitude | Elevation/m | No. trees | $\delta^{18}O_{soil}$/‰ | No. soil water replicates |
|---|---|---|---|---|---|---|
| 1 | 54° 56′ 37″ S | 67° 39′ 25″ W | 29 | 5 | −11.5 ± 0.25 | 3 |
| 2 | 54° 57′ 04″ S | 67° 38′ 58″ W | 97 | 4 | −13.1 ± 0.73 | 4 |
| 3 | 54° 58′ 33″ S | 67° 40′ 22″ W | 247 | 5 | −10.5 ± 1.17 | 3 |
| 4 | 54° 59′ 19″ S | 67° 41′ 02″ W | 395 | 7 | −12.0 ± 1.29 | 2 |
| 5 | 54° 59′ 35″ S | 67° 41′ 04″ W | 527 | 11 | −12.0 ± 0.58 | 4 |

($^{13}C/^{12}C$) are expressed as $\delta^{13}C$ and reported relative to the Vienna Pee Dee Belemnite standard.

*2.3.1. Preservation of fossil material*

Exceptional preservation of the fossil *Nothofagus* utilised in this study is well documented (Francis and Hill, 1996), and is supported by scanning electron microscope imaging (Fig. 1D), which shows excellent retention of wood fibres. Although it is clear that some degradation of vessels has occurred, this should not impact the isotopic signal of the remaining cellulose; cellulose extracted from fossil trees significantly older than those used in this study (up to 53 Ma; Wolfe et al., 2012; Hook et al., 2014, 2015; Staccioli et al., 2014) was extracted in low yield (<5%; Hook et al., 2015) indicating a high degree of cellulose degradation, but showed no signs of isotopic alteration. Mineral contaminants in the form of microcrystalline calcite were detected in the Sirius Group fossil trees using energy dispersive X-ray spectroscopy, which could affect both $\delta^{18}O$ and $\delta^{13}C$, but the delignification step during extraction is performed below pH 5, which removed all calcite. After extraction, cellulose was recovered as a white fluffy material (5–30% yield), which is a clear indication that cellulose is well-preserved and hence the fossil material is appropriate for isotope analysis.

*2.3.2. Cellulose isotope measurements*

Cellulose was extracted from both modern and fossil samples using batch extraction equipment described by Wieloch et al. (2011). To summarise, ground wood samples were heated in aqueous NaOH solution (5%, 2 h, 60 °C, repeated twice) to remove tannins, resins and fatty acids. Samples were then heated (60 °C) in acidified $NaClO_2$ (via glacial acetic acid; 7.5%, pH 4–5) for 10 h; this step was repeated four times to ensure complete delignification. Finally, we used a solution of NaOH (17%; 60 °C, 2 h) to remove hemicelluloses, leaving α-cellulose for analysis. Cellulose samples were homogenised using a Retsch MM301 Mixer Mill, then freeze-dried for 24 h to remove ambient water. Samples were stored in Eppendorf vials and kept in a desiccator for >24 h prior to isotope analysis.

In order to measure $\delta^{18}O_{cell}$, the milled, freeze-dried cellulose samples were weighed, packed into silver capsules and pyrolysed at 1450 °C. Oxygen isotope ratios were measured using an elemental analyser with a purge and trap column (Elementar vario PYRO cube), coupled to an Isoprime isotope ratio-mass spectrometer. Ratios of $^{18}O/^{16}O$ were converted to $\delta^{18}O_{VSMOW}$ with a one point linear calibration using IAEA-601 (benzoic acid; $\delta^{18}O = 23.15 \pm 0.3‰$) with reference to cellulose from Sigma-Aldrich, UK (Lot#SLBD2972V; hereafter Leeds Sigma cellulose). The Leeds Sigma cellulose was analysed at the University of Leeds against IAEA-CH-3 cellulose, assuming $\delta^{18}O = 31.9 \pm 0.5‰$ (Hunsinger et al., 2010) and assigned a value of 29.2 ± 0.2. Standards were included at an interval of every twelve samples. Within-run reproducibility of an internal check standard was ±0.37‰. For $\delta^{13}C$ analysis, extracted cellulose samples were weighed and packed into tin capsules. Carbon isotope ratios were measured using an Elementar vario PYRO cube elemental analyser coupled to an Isoprime mass spectrometer. The encapsulated samples were combusted at 1150 °C in pure oxygen. Ratios of $^{13}C/^{12}C$ were calibrated to the international VPDB scale using in-house urea and C4 sucrose. These were assigned values of −46.83 ± 0.22‰ and −11.93 ± 0.24‰, respectively after calibration using six replicates of each of the following international standards: IAEA-LSVEC (−46.479‰), IAEA-CH7 (−31.83‰), IAEA-CH6 (−10.45‰) and IAEA-CO1 (+2.48‰). The precision obtained for repeat analysis was better than ±0.2‰ (σ).

*2.3.3. Water isotope measurements*

Water was extracted from roots and soils by cryogenic vacuum distillation, following the procedure detailed by West et al. (2006). Extracted samples, along with stream waters, were stored frozen until they were measured for water isotope ratios at the School of Environmental Sciences, University of East Anglia, UK. The $^{18}O/^{16}O$ ratios were analysed using a Picarro L1102-i cavity ring-down spectroscopy analyser with a CTC Analytics autosampler. Each sample was injected and measured 6 times using 2.5 μl of water for each injection. Together with the samples, two secondary international standards (USGS 64444 and USGS 67400) and one internal laboratory standard (NTW – Norwich tap water) were measured, each injected 10 times in order to minimize memory effects. Final isotopic compositions were calculated using the calibration line based on the secondary international standards and reported in permil units with respect to V-SMOW on the V-SMOW – SLAP scale. The precision of the measurements is 0.1‰ for $\delta^{18}O$.

The isotopic composition of plant source water for the modern *Nothofagus* in this study was constrained by measuring $\delta^{18}O$ of soil waters ($\delta^{18}O_{soil}$) for the five sites, which ranged between −13.1 ± 0.73‰ and −10.6 ± 1.17‰ (1 σ; grand mean = −11.9 ± 0.89‰; $n = 16$; Table 1). Oxygen isotopes from eight streams and lakes across the sampling transect ($\delta^{18}O_{stream}$), ranged between −11.1‰ and −9.8‰ (mean = −10.8 ± 0.41‰). Root water extracted from *Nothofagus* trees at three sites (mean = −10.5 ± 0.54‰, $n = 4$) was isotopically similar to $\delta^{18}O_{stream}$ and $\delta^{18}O_{precip}$, indicating that plants took up water from an annually integrated precipitation signal.

The $\delta^{18}O$ data presented here only represent one year's precipitation. We also used temperature, precipitation and precipitation $\delta^{18}O$ data from the nearby Global Network of Isotopes in Precipitation (GNIP) station at Ushaia, Argentina (54°46′48″ S; 68°16′48″ W), approximately 50 km away, in order to take into consideration summer and winter seasonal precipitation in this study, noting that there are a number of missing years for the data set; a more complete dataset is available from Punta Arenas but this station is significantly further away. Mean summer precipitation for Ushaia was −9.9 ± 0.9‰; mean winter precipitation was −11.92 ± 0.75‰, which is not statistically different from the mean soil water $\delta^{18}O$ ($p < 0.001$).

*2.3.4. Modelling $\delta^{18}O_{source}$*

There are multiple models of varying complexity linking these parameters and it is not clear whether more complex models provide better predictions than simpler ones. For the purposes of this study, we used a relatively simple model given by Eq. (1) (Anderson et al., 2002), which was chosen because there are only two unconstrained parameters (relative humidity, RH, and the fraction of leaf water not subject to fractionation, *f*). We acknowledge that there are more complex process-based and mechanistic models described in the literature, but consider that the use of more complex models linking $\delta^{18}O_{source}$ with $\delta^{18}O_{cell}$ (Roden et al., 2000; Danis et al., 2012) would require making assumptions about a larger number of parameters which are difficult to constrain in deep time, for example amount of precipitation and daily max and min temperatures. The Anderson model has been used in multiple studies to reconstruct past precipitation isotopes (Csank et al., 2011; Wolfe et al., 2012; Hook et al., 2015).

$$\delta^{18}O_{source} = \delta^{18}O_{cell} - (1-f)(1-RH)(\varepsilon e + \varepsilon k) - \varepsilon \quad (1)$$

where ε is the biological fractionation factor associated with the formation of cellulose (+27 ± 3‰; Sternberg and DeNiro, 1983), εe is the equilibrium liquid-vapour fractionation for water and approximates $\delta^{18}O$ of atmospheric vapour (assumed here to be 11‰; Majoube, 1971) and the subscript *source* denotes source water. The kinetic liquid-vapour fractionation (εk) is dependent on leaf morphology and boundary layer vapour transport conditions; broad-leaf trees have quasi-laminar boundary layer conditions so εk = 21‰ (Buhay et al., 1996). The parameter *f* is the fraction of leaf water not subject to evaporation (Allison et al., 1985) and also includes the isotopic alteration of carbon-bound oxygen via exchange with stem water (Roden and Ehleringer, 1999).

We tested the assumptions made by Anderson et al. (2002) using measured $\delta^{18}O_{cell}$ from the modern analogue trees as input for the model (with RH = 0.7, $f = 0.2$ as in Allison et al., 1985) and compared

the results against measured $\delta^{18}O_{source}$ (i.e. soil and stream water) $\delta^{18}O_{root}$ from Isla Navarino, and the GNIP precipitation data from Ushaia. In order to apply the model to fossil *Nothofagus*, we applied a large range of values for RH that are consistent with measurements from high latitude modern analogue sites such as Isla Navarino (0.5–0.85) and using a random number generator with uniform distribution, we sampled between these constraints ($n = 10{,}000$) to provide an estimate of the possible range of $\delta^{18}O_{precip}$.

## 3. Results and discussion

### 3.1. Oxygen and carbon isotope ratios in modern Nothofagus

Oxygen and carbon isotope ratios in modern *Nothofagus* trees over a range of morphologies were measured to provide a first order check on the ability of fossil prostrate *Nothofagus* plants to record long-term climate and environmental variables. Mean $\delta^{18}O_{cell}$ for all sites over the sample period (1981–2011) ranged between 24.1‰ and 26.9‰. There was no statistically significant difference between the two Nothofagus species ($p > 0.7$; Student's unpaired *t*-test). However, there is also no statistically significant difference between sites for mean $\delta^{18}O_{cell}$, and therefore for altitude and morphology (i.e. prostrate or arboreal form), indicating that morphology does not impact absolute $\delta^{18}O_{cell}$ integrated over multiple tree rings. Intriguingly, prostrate trees in this study exhibit much lower inter-tree variability than their arborescent counterparts ($\sigma = 2.1‰$ and $\sigma = 0.8‰$, for arboreal and prostrate morphologies, respectively (Fig. 3)). Prostrate plants are more aerodynamically decoupled from the atmosphere, and retain tight control over their microclimate (Barrera et al., 2000; Korner, 2003), which may reduce inter-tree variability in transpiration.

Mean $\delta^{13}C_{cell}$ for each site ranged between −27.2‰ and −26.7‰ (grand mean = −26.6 ± 0.7‰), which is consistent with typical values for C3 land-plants (O'Leary, 1988). Mean inter-tree variability was low ($\sigma$ range = 0.6–0.8‰) and did not vary with altitude or morphology. In this case, $\delta^{13}C_{cell}$ variability may be dominated by carbon assimilation rather than stomatal conductance (in support of findings of Farquhar et al. (1998) and Scheidegger et al. (2000) for example). A dominant stomatal conductance signal would lead to co-varying carbon and oxygen isotope ratios with morphology (Lavergne et al., 2017a; Guerrieri et al., 2019).

The low EPS in this study means our chronology is inappropriate for studying climate variations at interannual resolution, and would need to be updated with more trees if that were the purpose of the study. However, this does not prevent us using the data to understand a longer-term integrated climate signal; the low inter-tree variability in the prostrate plants in particular suggests they may function well as a record of climate information integrated over longer timescales and we test this hypothesis using a physiological model below. This is particularly pertinent to the fossil plants in this study, where the tree ring widths are extremely narrow and do not provide sufficient material for analysis at annual resolution; data from the fossil plants is integrated over the entire individual plant.

### 3.2. Carbon isotopes in fossil Nothofagus

Mean $\delta^{13}C_{cell}$ was −22.6 ± 1.9‰ (1 $\sigma$). The inter-tree variability here is much larger than in either the arboreal or prostrate plants from Isla Navarino (−26.6 ± 0.7‰), which again is consistent with the dataset spanning millennial timescales. This range of values is significantly enriched by ~+4‰ ($p < 0.001$) relative to the mean values seen in the modern *Nothofagus* trees (Fig. 2).

Scarring on the bark (Francis and Hill, 1996) of the fossil plants implies strong winds and paleosol analysis suggests that MAP was 120–220 mm (Retallack et al., 2001), which is considerably lower than the MAP on Isla Navarino (400–500 mm). This would lead to enhanced water stress, although fossil *Nothofagus* leaves associated with the wood fragments are large in size indicating that the plants were not living in a marginal habitat (Hill et al., 1996) and thus any water stress could not have been too severe. For both fossil tree age scenarios, atmospheric $CO_2$ was equal to, or greater than present day, at ~400 ppm for the Pliocene, and exceeding 500 ppm for the warmest periods of the mid-Miocene (Pagani et al., 2010; Holbourn et al., 2015; Levy et al., 2016). Both of these factors would lead to enhanced water-use efficiency, reducing stomatal conductance and hence enriching $\delta^{13}C_{cell}$.

Additionally, Tipple et al. (2010) find that $\delta^{13}C$ of atmospheric $CO_2$ was higher than present day for both the Pliocene (between around −6.7 and −6‰) and mid-Miocene (between around −5.7 and −5‰), compared to between −8.5 and −7.5‰ for the present day (Keeling et al., 2017). This increase in the baseline $\delta^{13}C$ in combination with enhanced water-use efficiency, is sufficient to explain the large enrichment we see between modern and fossil $\delta^{13}C_{cell}$ data.

### 3.3. Source water $\delta^{18}O$ in modern Nothofagus

There was no significant trend in $\delta^{18}O$ of measured soil, root or stream waters with altitude, which is most likely because of the small altitude range covered in this study (0–600 m). Sites 2 and 3 $\delta^{18}O_{soil}$ are statistically different from each other ($p < 0.05$; one way ANOVA with post-hoc Tukey test) and site 2 is also significantly depleted relative to the stream and root water, suggesting an increased contribution

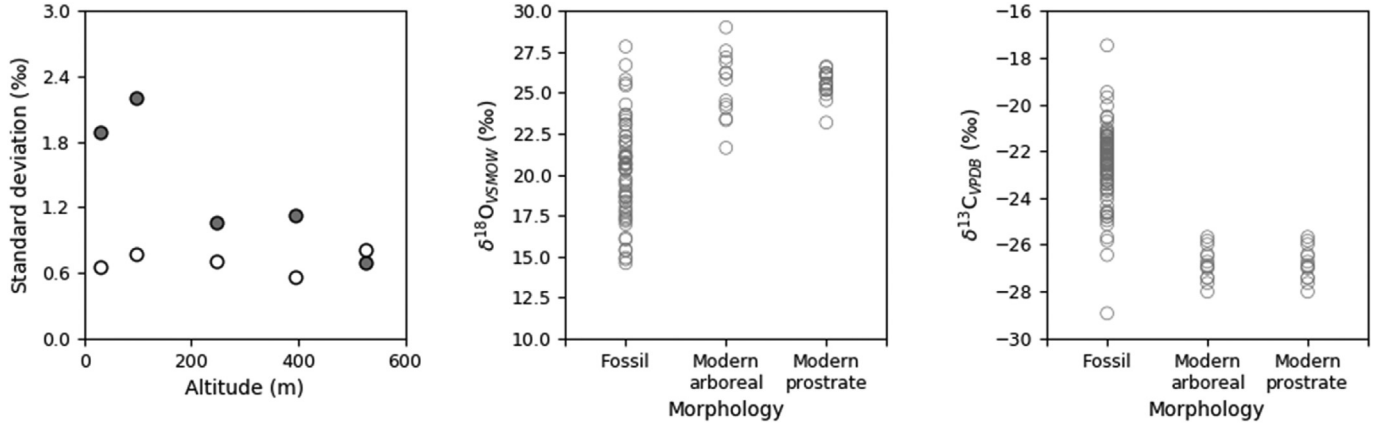


**Fig. 2.** (A) Standard deviation of $\delta^{13}C_{cell}$ (open circles) and $\delta^{18}O_{cell}$ (closed circles) with altitude for Nothofagus from Isla Navarino, demonstrating a decrease in variability for $\delta^{18}O_{cell}$ for prostrate trees. (B) Mean $\delta^{18}O_{cell}$ data for modern Nothofagus separated into arboreal and prostrate form, and fossil Nothofagus. (C) As panel (B) but for $\delta^{13}C_{cell}$.

from winter precipitation to soils. From these observations we infer that plant source water $\delta^{18}O$ ($\delta^{18}O_{source}$) can be treated as $\delta^{18}O_{precip}$, where $\delta^{18}O_{precip}$ is controlled by latitude, condensation temperature and precipitation amount (Dansgaard, 1964).

### 3.4. Source water $\delta^{18}O$ prediction from modern cellulose $\delta^{18}O$

We now test whether $\delta^{18}O_{precip}$ can be reconstructed from $\delta^{18}O_{cell}$, using the model from Anderson et al. (2002).

The chosen model under-predicted $\delta^{18}O_{source}$ by between 0.2‰ and 2.9‰ (mean for all sites = 1.5‰; Fig. 3). This could be due to model parametrization; we chose a value of exactly 27‰ for the biological fraction factor ε, but another value within the accepted range of 24–30‰ could equally be chosen (as in Anderson et al., 2002 and demonstrated by the *x*-axis error bars). Moreover, modelled $\delta^{18}O_{source}$ was not statistically different from $\delta^{18}O_{root}$, $\delta^{18}O_{stream}$ or GNIP summer precipitation, indicating that the model works well for predicting $\delta^{18}O_{precip}$ from measured $\delta^{18}O_{cell}$ in *Nothofagus*. We now apply the model to the fossil *Nothofagus* in order to calculate ancient $\delta^{18}O_{precip}$.

### 3.5. Reconstructing ancient precipitation $\delta^{18}O$ from fossil Nothofagus

Mean $\delta^{18}O_{cell}$ for the fossil plants was 20.3 ± 3.0‰. The inter-tree variability is similar in magnitude to that seen in modern trees, but is greater than the inter-tree variability seen in the prostrate plants of this study. It seems likely that these data capture both significant temporal variability and climate variability. It is important to note that here, we are treating all fossils as being geologically contemporaneous as they were all collected from the same bed, but it is highly likely that our data may span multiple millennia. Ice sheet fluctuations during both the mid-Miocene and Pliocene occurred at orbital timescales (Greenop et al., 2014; Patterson et al., 2014); therefore the duration represented by the fossils must be less than 100 kyr, but long enough for poorly developed soils to form and woody plants to colonise the area. This is consistent with the larger variability in the fossil data compared to the modern. Mean $\delta^{18}O_{cell}$ for the Sirius Group plant is significantly depleted by ~5‰ ($p < 0.001$) relative to the mean of the modern *Nothofagus* trees from Isla Navarino (25.5 ± 1.5‰). Broadly, there are two major controls on $\delta^{18}O_{cell}$, which could cause such an offset:

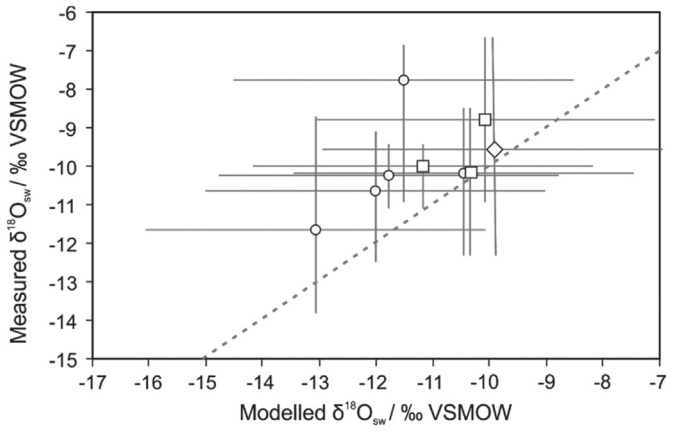


**Fig. 3.** The relationship between modelled source water $\delta^{18}O$ and measured $\delta^{18}O_{source}$ water for each site (from soils from each of the five sites (circles)), roots from three sites (squares) and Global Network of Isotopes in Precipitation $\delta^{18}O_{precip}$ (summer precipitation; diamond). Modelled source water $\delta^{18}O$ was calculated from measured $\delta^{18}O_{cell}$ (modern *Nothofagus*) using the same method as Anderson et al. (2002). Markers give the mean $\delta^{18}O$, y-error bars show the full measured data range, x-errors show the range of modelled $\delta^{18}O_{source}$ if ε were varied within the range given by Sternberg and DeNiro (1983), and a 1:1 ratio is given by the dotted line for comparison. Modelled data is calculated using RH = 0.7, $f = 0.2$.

evapotranspiration rates (controlled by relative humidity and stomatal conductance) and $\delta^{18}O$ of the plant's source water (McCarroll and Loader, 2004). From the modern data, we assume that plant source water is equal to precipitation $\delta^{18}O$ within the uncertainty of precipitation variability. In addition to latitude, precipitation amount, and temperature, there are further processes that could modify this signal, including evaporation from soil or plants using groundwater as a moisture source. Depletion could result from a large decrease in stomatal conductance caused by increased vapour pressure deficit reducing evapotranspiration from leaves. However, vapour pressure deficit across southern Chile is already relatively low (<0.5 kPa; Du et al., 2018) and it is unlikely that there would have been significant decreases in vapour pressure deficit for Antarctica when summer temperatures are not predicted to have been much lower (Rees-Owen et al., 2018). Alternatively, decreased $\delta^{18}O_{cell}$ could be caused by a difference in $\delta^{18}O_{precip}$, which is consistent with the higher palaeolatitude of the fossil plants (85°S for the Sirius Group, 54°S for Isla Navarino). We test this hypothesis using the physiological model for $\delta^{18}O_{precip}$ from Anderson et al. (2002). Using this approach, we calculate that mean continental Antarctic palaeoprecipitation was −16 ± 4.2‰ (1 σ; ranging between −26‰ and −3.5‰). Since $\delta^{18}O_{cell}$ is strongly modified by ambient relative humidity, the large range in our results is consistent with the conservative (i.e. wide) humidity range used in this study.

In the present day, $\delta^{18}O_{precip}$ over East Antarctica is highly variable, ranging from −55‰ at the highest elevations and furthest from the coast, to −25‰ near sea level at lower latitudes <75°S (Masson-Delmotte et al., 2008). However, there is considerable uncertainty surrounding the palaeoaltitude of the *Nothofagus* fossils sampled in this study (Ackert Jr. and Kurz, 2004), which makes it difficult to provide context for the reconstructed $\delta^{18}O_{precip}$ values. We therefore compared our record to measured Antarctic $\delta^{18}O_{precip}$ from sites above 75°S and less than 700 m above sea level (the height of the timberline on Isla Navarino; Masson-Delmotte et al., 2008), representing a reasonable habitat range. Reconstructed $\delta^{18}O_{precip}$ was significantly enriched by ~+12‰ relative to modern $\delta^{18}O_{precip}$ (ancient mean = −16‰, modern mean = −28‰; $p < 0.001$; Fig. 4). Growth experiments have suggested that plant $\delta^{2}H$ (and therefore by extension, $\delta^{18}O$) can be significantly enriched in plants grown under continuous light, analogous to the polar light regime (Yang et al., 2009). Therefore, part of the enrichment in the Sirius Group specimens could be accounted for by the continuous light regime experienced by the Antarctic plants during the growing season, which would increase $\delta^{18}O_{cell}$ via continuous transpiration, as opposed to the light regime on Isla Navarino, where plants undergo a diurnal transpiration-respiration cycle. However, the plants used by Yang et al. (2009) have a relatively high transpiration rate because of the relatively warm growing temperatures used in their experimental study. We suggest that the transpiration rate for the Sirius Group plants would likely be much lower because of the cold summer temperatures (~5 °C, compared to ~20 °C in the environment used by Yang et al., 2009). Furthermore, *Nothofagus* have been documented as having significantly tighter stomatal control of transpiration than co-existing conifers (Fernández et al., 2009), as used by Yang et al. (2009). Therefore it seems likely that there is much lower enrichment due to continuous light in the Sirius Group fossils (see Supplementary information for further discussion).

Our result has implications for regional and global climate during periods of ice sheet retreat in the Neogene. A significant enrichment in precipitation isotopes implies a considerable change in some of the atmospheric processes of the hydrological cycle. Plausible mechanisms include increased temperatures affecting fractionation during condensation, or changes in rainout patterns due to shifts in source moisture region or different atmospheric circulation patterns leading to a shortened vapour transport pathway. As previously discussed, warmer Antarctic temperatures (relative to today) are consistent with multiple contemporaneous terrestrial temperature proxies, which suggest that summer temperatures reached 5 °C during the period of study

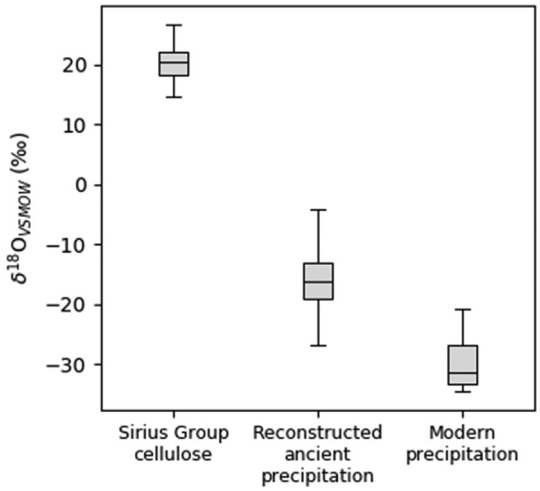


**Fig. 4.** Cellulose $\delta^{18}O$ from the Sirius Group fossil *Nothofagus*, with modelled $\delta^{18}O$ of palaeo precipitation and modern Antarctic snow. Modern measurements from Masson-Delmotte et al. (2008); data restricted to >75°S and below 700 masl. The median is given by the line, the first and third quartiles by the box, and the whiskers denote the full range of data.

(Ashworth and Kuschel, 2003; Ashworth and Preece, 2003; Ashworth and Cantrill, 2004; Rees-Owen et al., 2018). This result is also consistent with both age scenarios for the site: during both the mid-Miocene and Pliocene, sea surface temperatures in the Southern Ocean were several degrees warmer than today (Warny et al., 2009; McKay et al., 2012; Clark et al., 2013) and there is evidence for reduced sea ice cover (Whitehead et al., 2005; Warny et al., 2009). However, previous work by Feakins et al. (2012) suggests that the relationship between temperature and precipitation isotopes earlier in the Miocene (20–15 Ma) on the Antarctic coast was different from the modern, driven by increased evaporation from a warmer Southern Ocean. Similarly, isotopic disequilibrium between vapour and precipitation in modern-day Patagonia has been suggested to explain greater than expected $\delta^{18}O_{cell}$ (Penchenat et al., 2020). This implies that other factors may also influence the hydrological cycle at this time, which is plausible within the context of a warmer Neogene world, where warmer Southern Ocean temperatures could drive an increase in evaporation from high latitude moisture sources. Equally, the smaller ice sheet could well have influenced regional atmospheric circulation patterns, and changes in global atmospheric circulation are documented for the Pliocene (Brierley et al., 2009). These variables are likely to be important for understanding the full significance of our data, but are unconstrained, and a full exploration of hydrological changes is beyond the scope of this study. These questions could be more fully answered through further data collection to reduce proxy uncertainty, and the use of a coupled ocean-atmosphere climate model to investigate hydrodynamic changes.

## 4. Conclusions

By testing a simple physiological model linking $\delta^{18}O_{cell}$ with $\delta^{18}O_{precip}$ in two species of modern *Nothofagus* plants, which grow in both arboreal and prostrate form, we found that $\delta^{18}O_{cell}$ of prostrate *Nothofagus* faithfully records $\delta^{18}O_{precip}$ at multi- year resolution. Hitherto, most tree ring stable isotope analyses have been applied to trees with an arboreal habit in temperate and tropical environments. Therefore, it was previously unclear whether the assumptions made in tree ring isotope theory hold true for *krummholz*-type plants, such as those from Oliver Bluffs, which feature growth asymmetry that could affect isotopic signals via resource partitioning. Our findings demonstrate that prostrate trees are potentially suitable archives for recording climatological means over longer periods (on the order of decades). This result opens up high latitude and altitude end-member environments in both palaeo and modern times for tree ring isotope analysis.

The carbon isotope composition of cellulose from exceptionally well-preserved Neogene fossil wood from the Transantarctic Mountains, Antarctica was ~4‰ more positive than that of the modern samples. This difference is best explained as the result of a more positive value for the $\delta^{13}C$ of contemporaneous atmospheric $CO_2$ and enhanced water use efficiency at the Oliver Bluffs site, although the precise contribution of each of these factors to this signal is unknown.

The oxygen isotopic composition of the fossil wood provides new insights into Neogene hydrological cycling. Our record indicates that during a period of EAIS ice sheet retreat in which small prostrate shrubs colonised the exposed glacial landscape close to the South Pole, the hydrological cycle was markedly different to today with precipitation significantly enriched in $^{18}O$ by ~12‰ relative to modern precipitation over the continent. While the enrichment may be temperature driven alone, our result correlates well with the result of Feakins et al. (2012), suggesting that moisture source regions may have been different in the past. However, it is not possible to distinguish between these two possibilities, or some combination of both, based on the geochemical data alone.

## CRediT authorship contribution statement

**Rhian L. Rees-Owen:** Conceptualization, Methodology, Investigation, Formal analysis, Writing - original draft, Visualization. **Rob J. Newton:** Conceptualization, Methodology, Writing - review & editing. **Ruza F. Ivanovic:** Conceptualization, Writing - review & editing. **Jane E. Francis:** Conceptualization, Writing - review & editing. **James B. Riding:** Writing - review & editing. **Alina D. Marca:** Resources, Writing - review & editing.

## Declaration of competing interest

The authors declare that they have no known competing financial interests or personal relationships that could have appeared to influence the work reported in this paper.

## Acknowledgements

Many thanks are due to our two anonymous reviewers, whose detailed and helpful comments have helped to improve this manuscript. We thank F. Keay and A. Connolly of Leeds University for technical and analytical support, J. Forth for support in the field, and R. Brienen for equipment loans and useful discussions on sampling tree rings. R.L.R.O. thanks the Natural Environment Research Council (NERC) for supporting her PhD studentship (NE/K500847/1), the BGS for CASE support, and the Trans-Antarctic Association for support with fieldwork (TAA/13/10). R.I. was supported by a NERC Independent Fellowship (NE/K008536/1). J.B.R. publishes with the approval of the Executive Director, British Geological Survey (NERC). Fossil samples were obtained from A. Ashworth, North Dakota State University, and were collected during fieldwork for an NSF-funded project undertaken by A. Ashworth, J. Francis, D. Cantrill and S. Roof. Modern tree core samples were taken during the 2012-13 field season; thanks are due to Omora Ethnobotanical Park for permission to sample their trees and use their field station, as well as Marcelo Leppe at INACH for invaluable advice on conducting fieldwork in Chile.

## Appendix A. Supplementary data

Supplementary data to this article can be found online at https://doi.org/10.1016/j.scitotenv.2020.142247.

## References


Ackert Jr., R.P., Kurz, M.D., 2004. Age and uplift rates of Sirius Group sediments in the Dominion Range, Antarctica, from surface exposure dating and geomorphology. Glob. Planet. Chang. 42, 207–225. https://doi.org/10.1016/j.gloplacha.2004.02.001.

Aggarwal, P.K., et al., 2012. Stable isotopes in global precipitation: a unified interpretation based on atmospheric moisture residence time. Geophys. Res. Lett. 39 (11). https://doi.org/10.1029/2012GL051937 p. n/a-n/a.

Allison, G.B., Gat, J.R., Leaney, F.W.J., 1985. The relationship between deuterium and oxygen-18 delta values in leaf water. Chemical Geology (Isotope Geoscience Section) 58, 145–156.

Anderson, W.T., et al., 2002. Model evaluation for reconstructing the oxygen isotopic composition in precipitation from tree ring cellulose over the last century. Chem. Geol. 182 (2–4), 121–137. https://doi.org/10.1016/S0009-2541(01)00285-6.

Arens, N.C., Jahren, A.H., Amundson, R., 2000. Can C3 plants faithfully record the carbon isotopic composition of atmospheric carbon dioxide? Paleobiology 26 (1), 137–164. https://doi.org/10.1666/0094-8373(2000)026<0137:ccpfrt>2.0.co;2.

Ashworth, A.C., Cantrill, D.J., 2004. Neogene vegetation of the Meyer Desert Formation (Sirius Group) Transantarctic Mountains, Antarctica. Palaeogeogr. Palaeoclimatol. Palaeoecol. 213 (1–2), 65–82. https://doi.org/10.1016/j.palaeo.2004.07.002.

Ashworth, A.C., Kuschel, G., 2003. Fossil weevils (Coleoptera: Curculionidae) from latitude 85°S Antarctica. Palaeogeogr. Palaeoclimatol. Palaeoecol. 191 (2), 191–202. https://doi.org/10.1016/S0031-0182(02)00712-5.

Ashworth, A.C., Preece, R.C., 2003. The first freshwater molluscs from Antarctica. Journal Molluscan Studies 69 (1), 89–92. https://doi.org/10.1093/mollus/69.1.89.

Austermann, J., et al., 2015. The impact of dynamic topography change on Antarctic ice sheet stability during the mid-Pliocene warm period. Geology 43 (10), 927–930. https://doi.org/10.1130/G36988.1.

Baldini, L.M., et al., 2008. Spatial variability in the European winter precipitation δ 18 O-NAO relationship: implications for reconstructing NAO-mode climate variability in the Holocene. Geophys. Res. Lett. 35 (4), L04709. https://doi.org/10.1029/2007GL032027.

Ballantyne, A.P., et al., 2006. Pliocene Arctic temperature constraints from the growth rings and isotopic composition of fossil larch. Palaeogeogr. Palaeoclimatol. Palaeoecol. 242 (3–4), 188–200.

Ballantyne, A.P., et al., 2010. Significantly warmer Arctic surface temperatures during the Pliocene indicated by multiple independent proxies. Geology 38 (7), 603–606. https://doi.org/10.1130/G30815.1.

Barrera, M.D., et al., 2000. Structural and functional changes in Nothofagus pumilio forests along an altitudinal gradient in Tierra del Fuego, Argentina. J. Veg. Sci. 11, 179–188. https://doi.org/10.2307/3236797.

Barrett, P.J., 2013. Resolving views on Antarctic Neogene glacial history – the Sirius debate. Earth and Environmental Science Transactions of the Royal Society of Edinburgh 104 (May 2013), 31–53. https://doi.org/10.1017/S175569101300008X.

Battipaglia, G., et al., 2013. Elevated CO2 increases tree-level intrinsic water use efficiency: insights from carbon and oxygen isotope analyses in tree rings across three forest FACE sites. New Phytol. 197 (2), 544–554. https://doi.org/10.1111/nph.12044.

Beerling, D.J., 1996. Ecophysiological responses of woody plants to past CO2 concentrations. Tree Physiol. 16 (4), 389–396. https://doi.org/10.1093/treephys/16.4.389.

Brienen, R.J.W., et al., 2012. Oxygen isotopes in tree rings are a good proxy for Amazon precipitation and El Nino-southern oscillation variability. Proc. Natl. Acad. Sci. 109 (42), 16957–16962. https://doi.org/10.1073/pnas.1205977109.

Brierley, C.M., et al., 2009. Greatly expanded tropical warm pool and weakened Hadley circulation in the Early Pliocene. Science 323 (5922).

Buhay, W.M., Edwards, T.W.D., Aravena, R., 1996. Evaluating kinetic fractionation factors used for ecologic and paleoclimatic reconstructions from oxygen and hydrogen isotope ratios in plant water and cellulose. Geochim. Cosmochim. Acta 60 (12), 2209–2218. https://doi.org/10.1016/0016-7037(96)00073-7.

Buras, A., Wilmking, M., 2014. Straight lines or eccentric eggs? A comparison of radial and spatial ring width measurements and its implications for climate transfer functions. Dendrochronologia 32 (4), 313–326. https://doi.org/10.1016/j.dendro.2014.07.002 Elsevier GmbH.

Burckle, L.H., Potter, N., 1996. Pliocene-Pleistocene diatoms in Paleozoic and Mesozoic sedimentary and igneous rocks from Antarctica: a Sirius problem solved Pliocene-Pleistocene diatoms in Paleozoic and Mesozoic sedimentary and igneous rocks from Antarctica: a Sirius problem solved. Geology 24, 235–238. https://doi.org/10.1130/0091-7613(1996)024<0235.

Carlquist, S., 1987. Pliocene Nothofagus wood from the Transantarctic mountains. Aliso 11, 571–583.

Cernusak, L.A., English, N.B., 2014. Beyond tree-ring widths: stable isotopes sharpen the focus on climate responses of temperate forest trees. Tree Physiol. 35 (1), 1–3. https://doi.org/10.1093/treephys/tpu115.

Cernusak, L.A., et al., 2007. Transpiration efficiency of a tropical pioneer tree (Ficus insipida) in relation to soil fertility. J. Exp. Bot. 58 (13), 3549–3566. https://doi.org/10.1093/jxb/erm201.

Cernusak, L.A., Winter, K., Turner, B.L., 2009. Physiological and isotopic (δ13C and δ18O) responses of three tropical tree species to water and nutrient availability. Plant Cell Environ. 32 (10), 1441–1455. https://doi.org/10.1111/j.1365-3040.2009.02010.x.

Clark, N.A., et al., 2013. Fossil proxies of near-shore sea surface temperatures and seasonality from the late Neogene Antarctic shelf. Naturwissenschaften 100, 699–722. https://doi.org/10.1007/s00114-013-1075-9.

Cook, C.P., et al., 2013. Dynamic behaviour of the East Antarctic ice sheet during Pliocene warmth. Nat. Geosci. 6 (9), 765–769. https://doi.org/10.1038/ngeo1889.

Cook, E.R., Krusic, P.J., 2014. ARSTAN version 44h3: A tree-ring standardization program based on detrending and autoregressive time series modeling, with interactive graphics. Tree-Ring Laboratory, Lamont-Doherty Earth Observatory of Columbia University, Palisades, New York, USA. https://www.ldeo.columbia.edu/tree-ring-laboratory/resources/software.

Csank, A.Z., et al., 2011. Climate variability in the Early Pliocene Arctic: annually resolved evidence from stable isotope values of sub-fossil wood, Ellesmere Island, Canada. Palaeogeogr. Palaeoclimatol. Palaeoecol. 308 (3–4), 339–349.

Cullen, L.E., Grierson, P.F., 2009. Multi-decadal scale variability in autumn-winter rainfall in south-western Australia since 1655 AD as reconstructed from tree rings of Callitris columellaris. Clim. Dyn. 33 (2–3), 433–444. https://doi.org/10.1007/s00382-008-0457-8.

Danis, P.-A., et al., 2012. MAIDENiso: a multiproxy biophysical model of tree-ring width and oxygen and carbon isotopes. Can. J. For. Res. 42 (9), 1697–1713. https://doi.org/10.1139/x2012-089.

Dansgaard, W., 1964. Stable isotopes in precipitation. Tellus 16 (4), 436–468. https://doi.org/10.3402/tellusa.v16i4.8993.

Daux, V., et al., 2018. Comparisons of the performance of δ 13 C and δ 18 O of Fagus sylvatica, Pinus sylvestris, and Quercus petraea in the record of past climate variations. Journal of Geophysical Research: Biogeosciences 123 (4), 1145–1160. https://doi.org/10.1002/2017JG004203.

Dolan, A.M., et al., 2011. Sensitivity of Pliocene ice sheets to orbital forcing. Palaeogeogr. Palaeoclimatol. Palaeoecol. 309 (1), 98–110. https://doi.org/10.1016/j.palaeo.2011.03.030.

Du, J., et al., 2018. Global satellite retrievals of the near-surface atmospheric vapor pressure deficit from AMSR-E and AMSR2. Remote Sens. 10 (8), 1175. https://doi.org/10.3390/rs10081175.

Ehleringer, J.R., et al., 1986. Leaf carbon isotope and mineral composition in subtropical plants along an irradiance cline. Oecologia 70 (4), 520–526. https://doi.org/10.1007/BF00379898.

Farquhar, G.D., Gan, K.S., 2003. On the progressive enrichment of the oxygen isotopic composition along a leaf. Plant Cell Environment 26 (6), 801–819.

Farquhar, G.D., Ehleringer, J.R., Hubick, K.T., 1989. Carbon isotope discrimination and photosynthesis. Annu. Rev. Plant Physiol. Plant Mol. Biol. 40, 503–537.

Farquhar, G.D., Barbour, M.M., Henry, B.K., 1998. Interpretation of oxygen isotope composition of leaf material. Stable Isotopes: Integration of Biological, Ecological, and Geochemical Processes 27–48.

Feakins, Sarah J., Warny, S., Lee, J., 2012. Hydrologic cycling over Antarctica during the middle Miocene warming. Nature Geoscience. Nature Publishing Group 5 (8), 557–560. https://doi.org/10.1038/ngeo1498.

Fernández, M.E., Gyenge, J., Schlichter, T., 2009. Water flux and canopy conductance of natural versus planted forests in Patagonia, South America. Trees - Structure and Function 23 (2), 415–427. https://doi.org/10.1007/s00468-008-0291-y.

Fielding, C.R., et al., 2012. Neogene stratigraphy of Taylor Valley, Transantarctic Mountains, Antarctica: evidence for climate dynamism and a vegetated Early Pliocene coastline of McMurdo Sound. Glob. Planet. Chang. 96–97, 97–104. https://doi.org/10.1016/j.gloplacha.2010.09.003.

Francis, J.E., Hill, R.S., 1996. Fossil plants from the Pliocene Sirius Group, transantarctic evidence for mountains: climate from growth rings and fossil leaves. PALAIOS 11 (4), 389–396.

Gagen, M., et al., 2007. Exorcising the 'segment length curse': summer temperature reconstruction since AD 1640 using non-detrended stable carbon isotope ratios from pine trees in northern Finland. The Holocene 17 (4), 435–446. https://doi.org/10.1177/0959683607077012.

Gasson, E., et al., 2016. Dynamic Antarctic ice sheet during the early to mid-Miocene. Proc. Natl. Acad. Sci. (34), 201516130 https://doi.org/10.1073/pnas.1516130113.

Gessler, A., et al., 2007. Oxygen isotope enrichment of organic matter in Ricinus communis during the diel course and as affected by assimilate transport. New Phytol. 174 (3), 600–613. https://doi.org/10.1111/j.1469-8137.2007.02007.x.

Gessler, A., et al., 2009. Tracing carbon and oxygen isotope signals from newly assimilated sugars in the leaves to the tree-ring archive. Plant Cell Environ. 32 (7), 780–795. https://doi.org/10.1111/j.1365-3040.2009.01957.x.

Gessler, A., et al., 2014. Stable isotopes in tree rings: towards a mechanistic understanding of isotope fractionation and mixing processes from the leaves to the wood. Tree Physiol. 00, 1–23. https://doi.org/10.1093/treephys/tpu040.

Greenop, R., et al., 2014. Middle Miocene climate instability associated with high-amplitude CO2 variability. Paleoceanography 29 (9), 845–853. https://doi.org/10.1002/2014PA002653.

Griener, K.W., et al., 2015. Early to middle Miocene vegetation history of Antarctica supports eccentricity-paced warming intervals during the Antarctic icehouse phase. Glob. Planet. Chang. 127, 67–78. https://doi.org/10.1016/j.gloplacha.2015.01.006 Elsevier B.V.

Grießinger, J., et al., 2018. Imprints of climate signals in a 204 year δ18O tree-ring record of nothofagus pumilio from Perito Moreno Glacier, Southern Patagonia (50°S). Front. Earth Sci. 6 (April), 1–17. https://doi.org/10.3389/feart.2018.00027.

Grissino-Mayer, H.D., 2001. Evaluating Crossdating Accuracy: A Manual and Tutorial for the Computer Program COFECHA.

Guerrieri, R., et al., 2019. Disentangling the role of photosynthesis and stomatal conductance on rising forest water-use efficiency. Proc. Natl. Acad. Sci. 116 (34), 16909–16914. https://doi.org/10.1073/pnas.1905912116.

Hantemirov, R., Shiyatov, S., Gorlanova, L., 2011. Dendroclimatic study of Siberian juniper. Dendrochronologia 29 (2), 119–122. https://doi.org/10.1016/j.dendro.2010.05.001.

Hare, V.J., et al., 2018. Atmospheric CO2 effect on stable carbon isotope composition of terrestrial fossil archives. Nat. Commun. 9 (1), 252. https://doi.org/10.1038/s41467-017-02691-x.

Harwood, D.M., 1986. Diatom Biostratigraphy and Paleoecology With a Cenozoic History of Antarctic Ice Sheets. Ohio State University.
Hill, R.S., Jordan, G.J., 1996. Macrofossils as indicators of Plio-Pleistocene climates in Tasmaniaand Antarctica. Pap. Proc. R. Soc. Tasmania 130 (2), 9–15.
Hill, S.A., et al., 1995. Rapid recycling of triose phosphates in oak stem tissue. Plant Cell Environ. 18 (8), 931–936.
Hill, R.S., Harwood, D.M., Webb, P.-N., 1996. Nothofagus beardmorensis (Nothofagaceae), a new species based on leaves from the Pliocene Sirius Group, Transantarctic Mountains, Antarctica. Rev. Palaeobot. Palynol. 94, 11–24.
Holbourn, A., et al., 2015. Global perturbation of the carbon cycle at the onset of the Miocene Climatic Optimum. Geology 43 (2), 123–126. https://doi.org/10.1130/G36317.1.
Holmes, R.L., 1983. Computer-assisted quality control in tree-ring dating and measurement. Tree-Ring Bull. 43 (1), 69–78.
Hook, B.A., et al., 2014. Stable isotope paleoclimatology of the earliest Eocene using kimberlite-hosted mummified wood from the Canadian Subarctic. Biogeosci. Discuss. 11 (11), 16269–16308. https://doi.org/10.5194/bgd-11-16269-2014.
Hook, B.A., et al., 2015. Extraction of α-cellulose from mummified wood for stable isotopic analysis. Chem. Geol. 405, 19–27. https://doi.org/10.1016/j.chemgeo.2015.04.003.
Hunsinger, G.B., Hagopian, W.M., Jahren, A.H., 2010. Offline oxygen isotope analysis of organic compounds with high N:O. Rapid Commun. Mass Spectrom. 24 (21), 3182–3186. https://doi.org/10.1002/rcm.4752.
Jahren, A.H., Sternberg, L.S.L., 2008. Annual patterns within tree rings of the Arctic middle Eocene (ca. 45 Ma): isotopic signatures of precipitation, relative humidity, and deciduousness. Geology 36 (2), 99–102. https://doi.org/10.1130/G23876a.1.
Jahren, A.H., et al., 2001. Terrestrial record of methane hydrate dissociation in the Early Cretaceous. Geology 29 (2), 159–162. https://doi.org/10.1130/0091-7613(2001)029<0159:TROMHD>2.0.CO.
Jahren, A.H., et al., 2009. The environmental water of the middle Eocene Arctic: evidence from δD, δ18O and δ13C within specific compounds. Palaeogeogr. Palaeoclimatol. Palaeoecol. 271 (1–2), 96–103. https://doi.org/10.1016/j.palaeo.2008.09.016 Elsevier B.V.
Keeling, R.F., et al., 2017. Atmospheric evidence for a global secular increase in carbon isotopic discrimination of land photosynthesis. Proc. Natl. Acad. Sci. 114 (39), 10361–10366. https://doi.org/10.1073/pnas.1619240114.
Köhler, I.H., et al., 2010. Intrinsic water-use efficiency of temperate seminatural grassland has increased since 1857: an analysis of carbon isotope discrimination of herbage from the Park Grass Experiment. Glob. Chang. Biol. 16 (5), 1531–1541. https://doi.org/10.1111/j.1365-2486.2009.02067.x.
Korner, C., 2003. Plant ecology at high elevations. Alpine Plant Life: Functional Plant Ecology of High Mountain Ecosystems, pp. 1–7.
Kress, A., et al., 2010. A 350 year drought reconstruction from alpine tree ring stable isotopes. Glob. Biogeochem. Cycles 24 (2). https://doi.org/10.1029/2009GB003613 n/a-n/a.
Labuhn, I., et al., 2016. French summer droughts since 1326 CE: a reconstruction based on tree ring cellulose δ 18 O. Clim. Past 12 (5), 1101–1117. https://doi.org/10.5194/cp-12-1101-2016.
Lavergne, A., et al., 2016. Are the oxygen isotopic compositions of Fitzroya cupressoides and Nothofagus pumilio cellulose promising proxies for climate reconstructions in northern Patagonia? Journal of Geophysical Research: Biogeosciences https://doi.org/10.1002/2015JG003260 p. n/a-n/a.
Lavergne, A., Daux, V., et al., 2017a. Improvement of isotope-based climate reconstructions in Patagonia through a better understanding of climate influences on isotopic fractionation in tree rings. Earth Planet. Sci. Lett. 459, 372–380. https://doi.org/10.1016/j.epsl.2016.11.045.
Lavergne, A., Gennaretti, F., et al., 2017b. Modelling tree ring cellulose d18O variations in two temperature-sensitive tree species from North and South America. Clim. Past 13 (11), 1515–1526. https://doi.org/10.5194/cp-13-1515-2017.
Lavergne, A., et al., 2018. Past summer temperatures inferred from dendrochronological records of *Fitzroya cupressoides* on the eastern slope of the Northern Patagonian Andes. Journal of Geophysical Research: Biogeosciences 123 (1), 32–45. https://doi.org/10.1002/2017JG003989.
Lawver, L.A., Gahagan, L.M., 2003. Evolution of Cenozoic seaways in the circum-Antarctic region. Palaeogeogr. Palaeoclimatol. Palaeoecol. 198 (1–2), 11–37. https://doi.org/10.1016/S0031-0182(03)00392-4.
Levy, R.H., et al., 2016. Antarctic ice sheet sensitivity to atmospheric CO2 variations in the early to mid-Miocene. Proc. Natl. Acad. Sci. 113 (13), 3453–3458. https://doi.org/10.1073/pnas.1516030113.
Majoube, M., 1971. Oxygen-18 and deuterium fractionation between water and steam. Journal de Chimie Physique et de Physico-Chimie Biologique 68 (10), 1423.
Masson-Delmotte, V., et al., 2008. A review of Antarctic surface snow isotopic composition: observations, atmospheric circulation, and isotopic modeling*. J. Clim. 21 (13), 3359–3387. https://doi.org/10.1175/2007JCLI2139.1.
McCarroll, D., Loader, N.J., 2004. Stable isotopes in tree rings. Quat. Sci. Rev. 23, 771–801.
McKay, R.M., et al., 2012. Antarctic and Southern Ocean influences on Late Pliocene global cooling. Proc. Natl. Acad. Sci. U. S. A. 109 (17), 6423–6428. https://doi.org/10.1073/pnas.1112248109.
McKelvey, B.C., et al., 1991. The Dominion Range Sirius Group: a record of the late Pliocene-early Pleistocene Beardmore Glacier. Geological Evolution of Antarctica 675–682.
Mercer, J.H., 1986. Southernmost Chile: a modern analog of the southern shores of the Ross Embayment during Pliocene warm intervals. Antarct. J. US 21 (5), 103–105.
Moore, D.M., 1983. Flora of Tierra del Fuego. Anthony Nelson, Oswesrty.
Nabeshima, E., et al., 2018. Seasonal changes of δD and δ18O in tree-ring cellulose of Quercus crispula suggest a change in post-photosynthetic processes during early-wood growth. In: Mencuccini, M. (Ed.), Tree Physiology. vol. 38, pp. 1829–1840. https://doi.org/10.1093/treephys/tpy068 (12).
Naulier, M., et al., 2014. Carbon and oxygen isotopes of lakeshore black spruce trees in northeastern Canada as proxies for climatic reconstruction. Chem. Geol. 374–375, 37–43. https://doi.org/10.1016/j.chemgeo.2014.02.031.
Offerman, C., et al., 2011. The long way down - are carbon and oxygen isotope signals in the tree ring uncoupled from canpoy physiological processes? Tree Physiol. 31 (10), 1088–1102.
Ogée, J., et al., 2003. MuSICA, a CO2, water and energy multilayer, multileaf pine forest model: evaluation from hourly to yearly time scales and sensitivity analysis. Glob. Chang. Biol. 9 (5), 697–717. https://doi.org/10.1046/j.1365-2486.2003.00628.x.
Ogée, J., et al., 2009. A single-substrate model to interpret intra-annual stable isotope signals in tree-ring cellulose. Plant Cell Environ. 32 (8), 1071–1090. https://doi.org/10.1111/j.1365-3040.2009.01989.x.
Ohneiser, C., et al., 2020. Warm fjords and vegetated landscapes in early Pliocene East Antarctica. Earth Planet. Sci. Lett. 534, 116045. https://doi.org/10.1016/j.epsl.2019.116045 Elsevier B.V.
O'Leary, M.H., 1988. Carbon isotopes in photosynthesis. BioScience 38 (5), 328–336.
Pagani, M., et al., 2010. High Earth-system climate sensitivity determined from Pliocene carbon dioxide concentrations. Nat. Geosci. 3 (1), 27–30. https://doi.org/10.1038/ngeo724 Nature Publishing Group.
Patterson, M.O., et al., 2014. Orbital forcing of the East Antarctic ice sheet during the Pliocene and Early Pleistocene. Nat. Geosci. 7 (11), 841–847. https://doi.org/10.1038/ngeo2273.
Penchenat, T., et al., 2020. Isotopic equilibrium between precipitation and water vapor in Northern Patagonia and its consequences on δ 18 O cellulose estimate. Journal of Geophysical Research: Biogeosciences 125 (3). https://doi.org/10.1029/2019JG005418.
Pollard, D., Deconto, R.M., 2016. Contribution of Antarctica to past and future sea-level rise. Nature. Nature Publishing Group 531 (7596), 591–597. https://doi.org/10.1038/nature17145.
Pollard, D., Deconto, R.M., Alley, R.B., 2015. Potential Antarctic Ice Sheet retreat driven by hydrofracturing and ice cliff failure. Earth Planet. Sci. Lett. 412, 112–121. https://doi.org/10.1016/j.epsl.2014.12.035 Elsevier B.V.
Pound, M.J., et al., 2012. Global vegetation dynamics and latitudinal temperature gradients during the Mid to Late Miocene (15.97–5.33Ma). Earth Sci. Rev. 112 (1–2), 1–22. https://doi.org/10.1016/j.earscirev.2012.02.005.
Priault, P., Wegener, F., Werner, C., 2009. Pronounced differences in diurnal variation of carbon isotope composition of leaf respired CO2 among functional groups. New Phytol. 181 (2), 400–412. https://doi.org/10.1111/j.1469-8137.2008.02665.x.
Rees-Owen, R.L., et al., 2018. The last forests on Antarctica: reconstructing flora and temperature from the Neogene Sirius Group, Transantarctic Mountains. Org. Geochem. 118, 4–14. https://doi.org/10.1016/j.orggeochem.2018.01.001.
Retallack, G.J., Krull, E.S., Bockheim, J.G., 2001. New grounds for reassessing palaeoclimate of the Sirius Group, Antarctica. J. Geol. Soc. Lond. 158, 925–935.
Roden, J.S., Ehleringer, J.R., 1999. Observations of hydrogen and oxygen isotopes in leaf water confirm the Craig-Gordon model under wide-ranging environmental conditions. Plant Physiol. 120 (4), 1165–1174.
Roden, J.S., Ehleringer, J.R., 2000. Hydrogen and oxygen isotope ratios of tree ring cellulose for field-grown riparian trees. Oecologia 123 (4), 481–489. https://doi.org/10.1007/s004420000349.
Roden, J.S., Lin, G., Ehleringer, J.R., 2000. A mechanistic model for interpretation of hydrogen and oxygen isotope ratios in tree-ring cellulose. Geochim. Cosmochim. Acta 64 (1), 21–35. https://doi.org/10.1016/S0016-7037(99)00195-7.
Scheidegger, Y., et al., 2000. Linking stable oxygen and carbon isotopes with stomatal conductance and photosynthetic capacity: a conceptual model. Oecologia 125 (3), 350–357. https://doi.org/10.1007/s004420000466.
Schubert, B.A., Jahren, A.H., 2011. Quantifying seasonal precipitation using high-resolution carbon isotope analyses in evergreen wood. Geochim. Cosmochim. Acta 75 (22), 7291–7303. https://doi.org/10.1016/j.gca.2011.08.002.
Schubert, B.A., et al., 2012. A summertime rainy season in the Arctic forests of the Eocene. Geology 40 (6), 523–526. https://doi.org/10.1130/G32856.1.
Schulze, E.-D., et al., 1996. Rooting depth, water availability, and vegetation cover along an aridity gradient in Patagonia. Oecologia 108 (3), 503–511. https://doi.org/10.1007/BF00333727.
Sime, L.C., et al., 2009. Evidence for warmer interglacials in East Antarctic ice cores.', Nature. Nat. Publ. Group 462 (7271), 342–345. https://doi.org/10.1038/nature08564.
Staccioli, G., Santoni, I., Pizzo, B., 2014. Decay of fossil wood from kimberlite pipes of Lac de Gras in the Canadian sub-Arctic area. Annales de Paléontologie 100 (1), 87–94. https://doi.org/10.1016/j.annpal.2013.11.004.
Sternberg, L.S.L., DeNiro, M.J., 1983. Isotopic composition of cellulose from C3, C4, and CAM plants growing near one another. Science 220 (4600), 947–949. https://doi.org/10.1126/science.220.4600.947.
Sternberg, L., Ellsworth, P.F.V., 2011. Divergent biochemical fractionation, not convergent temperature, explains cellulose oxygen isotope enrichment across latitudes. PLoS One 6 (11), e28040. https://doi.org/10.1371/journal.pone.0028040 Edited by H. Y. H. Chen.
Sternberg, L.S.L., et al., 2006. Variation in oxygen isotope fractionation during cellulose synthesis: intramolecular and biosynthetic effects. Plant Cell Environ. 29 (10), 1881–1889.
Stokes, M.A., Smiley, T.L., 1968. An Introduction to Tree-Ring Dating. The University of Chicago Press, Chicago and London.
Stroeven, A.P., Prentice, M.L., Kleman, J., 1996. On marine microfossil transport and pathways in Antarctica during the late Neogene: evidence from the Sirius Group at Mount Fleming. Geology 24 (8), 727–730. https://doi.org/10.1130/0091-7613(1996)024<0727:OMMTAP>2.3.CO;2.
Switsur, V.R., et al., 1995. Stable isotope studies in tree rings from oak—techniques and some preliminary results. Paläoklimaforschung 15, 129–140.

Tipple, B.J., Meyers, S.R., Pagani, M., 2010. Carbon isotope ratio of Cenozoic CO2: a comparative evaluation of available geochemical proxies. Paleoceanography 25 (3). https://doi.org/10.1029/2009PA001851 p. n/a-n/a.

Treydte, K.S., et al., 2007. Signal strength and climate calibration of a European tree-ring isotope network. Geophys. Res. Lett. 34 (24), L24302. https://doi.org/10.1029/2007GL031106.

Treydte, K., et al., 2014. Seasonal transfer of oxygen isotopes from precipitation and soil to the tree ring: source water versus needle water enrichment. The New phytologist 202 (3), 772–783. https://doi.org/10.1111/nph.12741.

Warny, S., et al., 2009. Palynomorphs from a sediment core reveal a sudden remarkably warm Antarctica during the middle Miocene. Geology 37 (10), 955–958. https://doi.org/10.1130/G30139A.1.

Webb, P.N., Harwood, D.M., 1987. Terrestrial flora of the Sirius Formation: its significance for Late Cenozoic glacial history. Antarct. J. US 22 (4), 7–11.

Webb, P.-N., Harwood, D.M., 1993. Pliocene fossil Nothofagus (southern beech) from Antarctica: phytogeography, dispersal strategies, and survival in high latitude glacial-deglacial environments. Forest Development in Cold Climates, pp. 135–165.

Webb, P.N., et al., 1984. Geology Cenozoic marine sedimentation and ice-volume variation on the East Antarctic craton Cenozoic marine sedimentation and ice-volume variation on the East Antarctic craton. Geology 12 (5), 287–291. https://doi.org/10.1130/0091-7613(1984)12<287.

Werner, C., Gessler, A., 2011. Diel variations in the carbon isotope composition of respired CO2 and associated carbon sources: a review of dynamics and mechanisms. Biogeosciences 8 (9), 2437–2459. https://doi.org/10.5194/bg-8-2437-2011.

Werner, R.A., et al., 2011. Metabolic fluxes, carbon isotope fractionation and respiration - lessons to be learned from plant biochemistry. New Phytol. 191 (1), 10–15. https://doi.org/10.1111/j.1469-8137.2011.03741.x.

West, A.G., Patrickson, S.J., Ehleringer, J.R., 2006. Water extraction times for plant and soil materials used in stable isotope analysis. Rapid Commun. Mass Spectrom. 20 (8), 1317–1321. https://doi.org/10.1002/rcm.2456.

Whitehead, J.M., Wotherspoon, S., Bohaty, S.M., 2005. Minimal Antarctic sea ice during the Pliocene. Geology 33 (2), 137–140. https://doi.org/10.1130/G21013.1.

Wieloch, T., et al., 2011. A novel device for batch-wise isolation of α-cellulose from small-amount wholewood samples. Dendrochronologia 29 (2), 115–117. https://doi.org/10.1016/j.dendro.2010.08.008.

Wigley, T.M.L., Briffa, K.R., Jones, P.D., 1984. On the average value of correlated time series, with applications in dendroclimatology and hydrometeorology. J. Clim. Appl. Meteorol. 23 (2), 201–213. https://doi.org/10.1175/1520-0450(1984)023<0201:OTAVOC>2.0.CO;2.

Wolfe, A.P., et al., 2012. Pristine early eocene wood buried deeply in kimberlite from northern Canada. PLoS One 7 (9), e45537. https://doi.org/10.1371/journal.pone.0045537.

Woodcock, H., Bradley, R.S., 1994. Salix arctica (pall.): its potential for dendroclimatological studies in the High Arctic. Dendrochronologia 12, 11–22.

Xu, C., Sano, M., Nakatsuka, T., 2013. A 400-year record of hydroclimate variability and local ENSO history in northern Southeast Asia inferred from tree-ring δ18O. Palaeogeogr. Palaeoclimatol. Palaeoecol. 386, 588–598. https://doi.org/10.1016/j.palaeo.2013.06.025.

Xu, C., et al., 2016. Potential utility of tree ring δ 18 O series for reconstructing precipitation records from the lower reaches of the Yangtze River, southeast China. Journal of Geophysical Research: Atmospheres 121 (8), 3954–3968. https://doi.org/10.1002/2015JD023610.

Yakir, D., Sternberg, L.S.L., 2000. The Use of Stable Isotopes to Study Ecosystem Gas Exchange. (January). pp. 297–311.

Yang, H., et al., 2009. Carbon and hydrogen isotope fractionation under continuous light: implications for paleoenvironmental interpretations of the High Arctic during Paleogene warming. Oecologia 160 (3), 461–470. https://doi.org/10.1007/s00442-009-1321-1.

Zhu, M.F., et al., 2012. Indo-Pacific warm Pool convection and ENSO since 1867 derived from Cambodian pine tree cellulose oxygen isotopes. J. Geophys. Res.-Atmos., 117 doi:Artn D11307. https://doi.org/10.1029/2011jd017198.